

Analysis of methane and sulfate flux in methane-charged sediments from the Mississippi Canyon, Gulf of Mexico

Richard Coffin^{a,*}, Leila Hamdan^a, Rebecca Plummer^b, Joseph Smith^a, Joan Gardner^c, Rick Hagen^c, Warren Wood^d

^a Marine Biogeochemistry Section, Code 6114, Naval Research Laboratory, 4555 Overlook Avenue, S.W., Washington, DC 20375, USA

^b SAIC, NRL, Code 6114, Washington, DC, USA

^c NRL, Code 7420, Washington, DC, USA

^d NRL, Code 7432, Stennis, MS, USA

ARTICLE INFO

Article history:

Received 2 June 2007

Received in revised form 29 December 2007

Accepted 17 January 2008

Keywords:

Sediment
Methane hydrate
Sulfate
Chloride
Diffusion

ABSTRACT

Sediment porewater geochemical data (SO_4^{2-} , CH_4 , DIC, $\delta^{13}\text{C}$ -DIC and Cl^-) were obtained from piston cores collected in Atwater Valley, Gulf of Mexico, prior to 2005 drilling to study gas hydrates in the region. The geochemical data were used for a study of shallow sediment CH_4 cycling on a seafloor mound (mound F) where an apparent upward deflection of the bottom simulating reflector (BSR) suggested vertical fluid advection. Fifteen sediment cores, ranging from 300 to 800 cm long, were collected from locations on top of the mound and across a transect up to 3.5 km off the mound. The sulfate–methane transition (SMT) was determined in each core from porewater SO_4^{2-} and CH_4 concentration profiles and occurred at depths ranging from 0 to 410 cm below the seafloor (cmbsf). The shape of porewater SO_4^{2-} profiles plotted against depth also varied from linear to non-linear along the transect. Diffusion rates estimated from linear SO_4^{2-} concentration gradients ranged from -20.4 to $-249.1 \text{ mmol m}^{-2} \text{ a}^{-1}$ with the greatest rate measured in sediments on the mound. The large variation in SMT depth and SO_4^{2-} profiles along the transect indicates lateral differences in total vertical CH_4 flux between locations. Results suggest steady-state and non-steady-state CH_4 fluxes both on the mound and transitioning off the mound and likely differences in the relative contribution of fluid advection to local shallow sediment CH_4 cycling. Cores collected from on the mound had high porewater headspace CH_4 concentrations (up to 8.34 mM) coupled with elevated Cl^- concentrations (up to 956.5 mM) at shallow depths suggesting that salt diapirism in deep sediments may be inhibiting hydrate stability and increasing vertical CH_4 flux.

Published by Elsevier Ltd.

1. Introduction

Gas hydrates in ocean sediment and permafrost are being surveyed as a future source of unconventional natural gas (Milkov and Sassen, 2002). Compared to other fossil fuel reservoirs (e.g., coal, oil, and conventional natural gas), global gas hydrate deposits may contain twice the potential energy (Kvenvolden, 2000; Milkov et al., 2003). However, estimates of global oceanic gas hydrate deposits are highly variable, thus highlighting the need for a thorough inventory (Milkov and Sassen, 2001, 2002, 2003; Milkov et al., 2003).

Geochemical, geologic, and physical properties of marine sediments control hydrate stability and hence gas hydrate distribution.

Seismic surveys can provide evidence of gas hydrate deposits in regions where strong bottom simulating reflectors (BSRs) are observed (e.g., Hutchinson et al., 2008). Yet seismic surveys do not provide accurate quantification of deep sediment gas hydrate deposits nor identify gas hydrate deposits in regions where deeper free gas is absent (e.g., Paull et al., 1996; Cooper and Hart, 2003). In the Gulf of Mexico, BSRs are frequently absent in regions with active fluid vents and associated gas hydrates (e.g., Cooper and Hart, 2003), but can also be lacking where gas supplies are insufficient to support the formation of a BSR (e.g., Xu and Ruppel, 1999).

Since BSRs provide only indirect evidence of gas hydrate deposits, direct measurements of gas flux or the measurement of geochemical parameters in sediment porewaters can aid in interpreting seismic data (Borowski et al., 1999). Porewater SO_4^{2-} concentrations generally decrease with increasing depth in shallow sediment. In anoxic sediments SO_4^{2-} can be consumed as the terminal electron acceptor through organoclastic sulfate reduction (SR) during the decomposition of organic matter (Berner, 1964, 1978, 1980) or through the anaerobic oxidation of methane (AOM)

* Corresponding author. Tel.: +1 202 767 0065.

E-mail addresses: richard.coffin@nrl.navy.mil (R. Coffin), leila.hamdan@nrl.navy.mil (L. Hamdan), rebecca.plummer@nrl.navy.mil (R. Plummer), joseph.smith@nrl.navy.mil (J. Smith), gardner@nur.nrl.navy.mil (J. Gardner), rhagen@nur.nrl.navy.mil (R. Hagen), warren.wood@nrlssc.navy.mil (W. Wood).

(Borowski et al., 1999). Porewater SO_4^{2-} profiles in shallow sediments over deep hydrates are primarily dependent upon the sediment properties, which in turn control CH_4 vertical diffusion and advection rates, rates of organoclastic SR and AOM, the burial rate of terrestrial and planktonic organic matter, bioturbation and bioirrigation, and the downward diffusion of SO_4^{2-} from overlying seawater.

In many marine locations organoclastic SR is the dominant biogeochemical pathway for sediment sulfate consumption. However, in the presence of CH_4 , SR may be coupled with AOM (Borowski et al., 1999; Aharon and Fu, 2000; Orphan et al., 2001; Valentine, 2002; Valentine and Reeburgh, 2000). In sediments over CH_4 gas seeps and hydrates, maximum SR rates have been measured through the sulfate–methane transition (SMT); the sediment horizon where CH_4 and SO_4^{2-} coexist and where they are consumed during AOM (Borowski et al., 1999; Valentine, 2002). In these locations, AOM is conducted through a metabolic partnership between methanogen-like archaea that oxidize CH_4 and SO_4^{2-} reducing bacteria as described by a net reaction $\text{CH}_4 + \text{SO}_4^{2-} \rightarrow \text{HCO}_3^- + \text{HS}^- + \text{H}_2\text{O}$ (Orphan et al., 2001; Valentine, 2002). In sediments with vertical CH_4 flux, AOM may be the dominant pathway for SO_4^{2-} reduction (Borowski et al., 1996; Boetius et al., 2000; Pancost et al., 2000; Torres et al., 2002; Zhang et al., 2003; Treude et al., 2005). In such locations, the depth of the SMT and rates of AOM are controlled by the rate of vertical CH_4 flux (diffusive and advective) and downward SO_4^{2-} diffusion (Borowski et al., 1996, 1999). Quantifying lateral variations in SMT depths and SO_4^{2-} diffusion rates across features on the seafloor or in the subsurface (imaged by seismic data) can assist in locating marine CH_4 hydrate deposits (Borowski et al., 1999; Paull et al., 2005).

Using SMT depth and SO_4^{2-} profiles to identify locations with potentially significant CH_4 hydrate deposits assumes a steady-state inverse linear relationship between CH_4 and SO_4^{2-} , with organoclastic SR constant and the vertical SO_4^{2-} gradient varying as a function of the AOM rate (Borowski et al., 1996). Studies on Blake Ridge have interpreted the consistent location of a barium sulfate front underneath the SMT as evidence for steady-state conditions (Dickens, 2001; Riedinger et al., 2006). Physical and biological processes such as slope instability, fluid advection, bioturbation, pulsed inputs of organic matter, and SR not coupled to AOM can result in a non-steady-state relationship between SO_4^{2-} and CH_4 profiles. These and other factors can impact the validity of using SO_4^{2-} porewater profiles to predict vertical CH_4 flux (Hensen et al., 2003; Joye et al., 2004; Coffin et al., 2006a).

A more thorough understanding of the factors that control the shape of SO_4^{2-} and CH_4 profiles in marine sediments will contribute to evaluating SMT depth and SO_4^{2-} diffusion rates to assess deep sediment CH_4 flux and gas hydrate deposits. In this study, geochemical data are coupled with seismic and heat flow data (Coffin et al., 2005b, 2006b) to (1) contribute to understanding the connection between shallow seafloor geochemical data and seismic indicators of hydrate (e.g., BSRs); (2) study the biogeochemical factors that influence sediment porewater SO_4^{2-} profiles; and (3) elucidate the factors influencing geospatial variations in vertical CH_4 flux.

2. Materials and methods

2.1. Study location

This study was conducted at Atwater Valley in a shallow seafloor trough located in the Mississippi Canyon (Fig. 1). Piston coring was carried out in the vicinity of seafloor mounds F and D (Snyder et al., 2004) in lease blocks 13 and 14 (Fig. 1). Seafloor depths for the sampling area ranged from 1292 m to 1310 m with more shallow

regions measured upslope and on mound F and deeper locations between the mounds and down slope.

The study site lies within the Mississippi Fan fold belt, a 50-km-wide and 300-km-long area characterized by basinward-verging anticlines underlain by southern verging thrust faults (Weimer and Buffler, 1992). Folded sedimentary strata were deposited during Late Jurassic to Miocene time and in some regions are influenced by salt tongues and sheets (Weimer and Buffler, 1992). Shallow sediment overlying this geologic record contains a varied distribution of mounds and basins formed through physical actions in subsequent transport of sediments since the Late Cretaceous times (Ellwood et al., 2006). A result of this complex geologic formation is the distribution of small mounds created through vertical fluxes of hydrocarbons, mineral and methane rich fluidized sediments. The canyon fill that hosts the methane hydrate stability zone in this area is characterized by fine-grained sediments, mostly interbedded debris flows and hemipelagic sediments overlain by fine Holocene pelagic drape (Goodwin and Prior, 1989). This is consistent with the reports of fine-grained sediment recovered from drilling at this location (Claypool, 2006; Yun et al., 2006; Winters et al., 2008).

High-resolution seismic data were collected in the study area by the USGS (Hutchinson and Hart, 2004) and used to select the piston coring locations (Table 1). Additional seismic data were acquired using the Deep Towed Acoustic/Geophysics System (DTAGS) (Wood et al., 2002) towed 100–150 m above the seafloor. Available DTAGS data (Fig. 2) were used to describe structures below the sampling region that may influence fluid advection (Wood et al., 2008). This seismic profile showed a deep BSR away from mound F with a transition to a shallowing, “bell-shaped” BSR below mound F, indicating a thermal perturbation to the base of the HSZ that suggests upward fluid advection (Wood et al., 2008). Heat flow data across the coring region were consistent with shallowing of the seismic profile and the conclusion of upward fluid advection below mound F. Piston cores were collected along a 3.5 km transect between mounds D and F, located in the vicinity of 27.9356 °N, 89.2794 °W (Fig. 1). Near bottom photography through this study region found chemosynthetic communities on top of mound F but not at sites located off the mound (Hart et al., 2008).

2.2. Piston coring and core processing

Sediment cores were collected with a 2000 lb, 9-m-long piston coring device lined with 2.75" I.D. polycarbonate core barrels. Core positions were acoustically tracked using beacons on the deployment wire that provided 2–5 m station accuracy. After recovery, cores were cut in 10 cm whole round sections at 25–45 cm intervals. Sampling intervals were selected based on observations of dark (black) sediment and hydrogen sulfide odor, which are observational indicators of sulfide production associated with the SMT, and on the appearance of core gas pockets. Fewer samples were taken near the sediment–water interface and resolution was increased toward the suspected SMT depth. On average, 15 sediment sections were sampled from each core. Sediment plugs were collected from each section in a 3 ml polyethylene syringe with the end cut off and transferred to pre-weighed 20 ml serum vials to measure the headspace CH_4 concentrations (Hoehler et al., 2000). Approximately 5 g of wet sediment was sub-sampled from each section and collected in pre-weighed 31-mm snap-tight Petri-dishes to be frozen for laboratory measurements of sediment porosity and percent organic carbon.

Immediately after subsample collection, porewater was pressed from the remaining sediment from each section using 70 ml Reeburgh-style squeezers (Reeburgh, 1967) pressurized to ~400 kPa (~60 psi) by low-pressure air applied to a latex sheet placed between the core sections and gas inflow. Porewater was

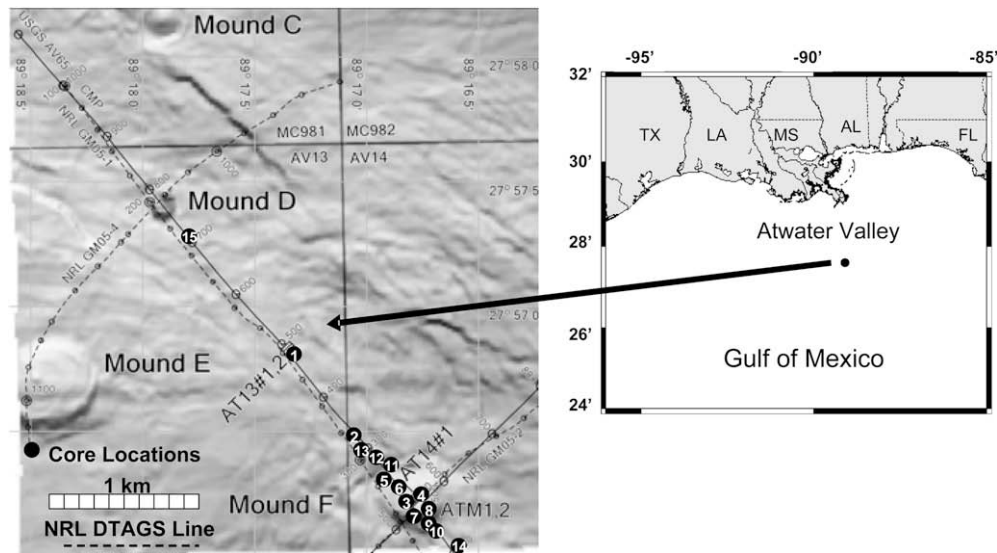


Fig. 1. Study site in Atwater Valley. Piston core locations were selected on, at the base and off mound F along the USGS high-resolution seismic line running between mounds D and F.

pre-filtered through Grade 1 qualitative filter paper into gas-tight 60-ml polypropylene syringes. Porewater was subsequently filtered through 0.2- μm Acrodisc PES syringe filters into ashed (4 h at 450 °C) 20 ml vials, then dispensed into 1–10 ml ashed vials for analysis. Pressed sediment was wrapped in ashed aluminum foil and stored frozen at -20 °C during transport to the land-based laboratory.

Methane (CH_4), sulfate (SO_4^{2-}) and chloride (Cl^-) concentrations were determined onboard ship. Analysis of dissolved inorganic carbon (DIC) concentrations and stable carbon isotope ratios ($\delta^{13}\text{C}$) was conducted at the land-based laboratory on samples held at -20 °C.

Sulfate and Cl^- concentrations were measured with a Dionex DX-120 ion chromatograph equipped with an AS-9HC column, Anion Self-Regenerating Suppressor (ASRS Ultra II), and an AS-40 autosampler (Paull et al., 2005). Samples were diluted 1:50 (vol/vol) and measured against diluted IAPSO standard seawater (28.9 mM SO_4^{2-} , 559 mM Cl^-). Analytical precision was $\pm 1\%$ of the standards.

Volumetric CH_4 gas concentrations were determined from the 3-ml sediment plugs using headspace techniques and were quantified against certified gas standards (Scott Gas) (Hoehler et al.,

2000). Concentration was calculated using sediment porosity and dry weight data obtained at the land-based laboratory (Hoehler et al., 2000). Analysis was performed using a Shimadzu 14-A gas chromatograph (GC) equipped with a flame ionization detector and Hayesep-Q 80/100 column. Gases were separated isothermally at 50 °C. True methane concentrations cannot be reliably measured from porewater samples because pressure reduction during core recovery lowers solubility and transfers dissolved CH_4 to the gas phase, hence, headspace CH_4 data presented below are used to provide data comparisons with SO_4^{2-} gradients.

Porewater DIC concentrations were measured using a UIC CO_2 coulometer and standardized to a certified seawater reference material (University of California, San Diego, CA). DIC conversion to CO_2 and separation from interfering sulfides was conducted according to Boehme et al. (1996). Dissolved inorganic carbon $\delta^{13}\text{C}$ were measured using a Thermo Delta Plus XP isotope ratio mass spectrometer (IRMS). Carbon dioxide was released into the headspace by adding 100 μl of 10% HCl into a DIC sample serum vial and transferred to the IRMS for $\delta^{13}\text{C}$ analysis. Stable carbon isotope ratios are presented in per mil units compared to a PeeDee Belenite standard.

Table 1

Locations, water depths, and penetration lengths of piston cores

Sample	LAT			LON			AV65 CMP	LON Dec deg	LAT Dec deg	Water depth (m)	Penetration length (m)
	Deg	Min	Sec	Deg	Min	Sec					
PC 1	27	56	48.8	89	17	21.6	487	89.28933	27.94689	1292	2.70
PC 2	27	56	28.644	89	17	6.629	344	89.28517	27.94129	1300	4.70
PC 3	27	56	15.738	89	16	49.969	219	89.28055	27.93771	1301	3.70
PC 4	27	56	14.534	89	16	47.732	205	89.27993	27.93737	1298	8.38
PC 5	27	56	20.137	89	16	53.121	250	89.28142	27.93893	1310	3.46
PC 6	27	56	17.797	89	16	51.937	236	89.28109	27.93828	1305	5.12
PC 7	27	56	11.508	89	16	47.356	190	89.27982	27.93653	1296	8.67
PC 8	27	56	9.514	89	16	46.247	178	89.27951	27.93598	1296	5.15
PC 9	27	56	6.189	89	16	43.101	150	89.27864	27.93505	1304	4.36
PC 10	27	56	2.437	89	16	40.942	125	89.27804	27.93401	1306	4.12
PC 11	27	56	21.998	89	16	55.766	264	89.28216	27.93944	1307	4.76
PC 12	27	56	24.084	89	16	56.983	285	89.2825	27.94002	1304	3.10
PC 13	27	56	28.378	89	17	0.924	17	89.28359	27.94122	1302	3.47
PC 14	27	55	56.881	89	16	32.79	70	89.27578	27.93247	1307	5.25
PC 15	27	57	20.066	89	17	50.963	737	89.29749	27.95557	1292	3.40

CMP number refers to USGS seismic line AV65 acquired in April 2003.

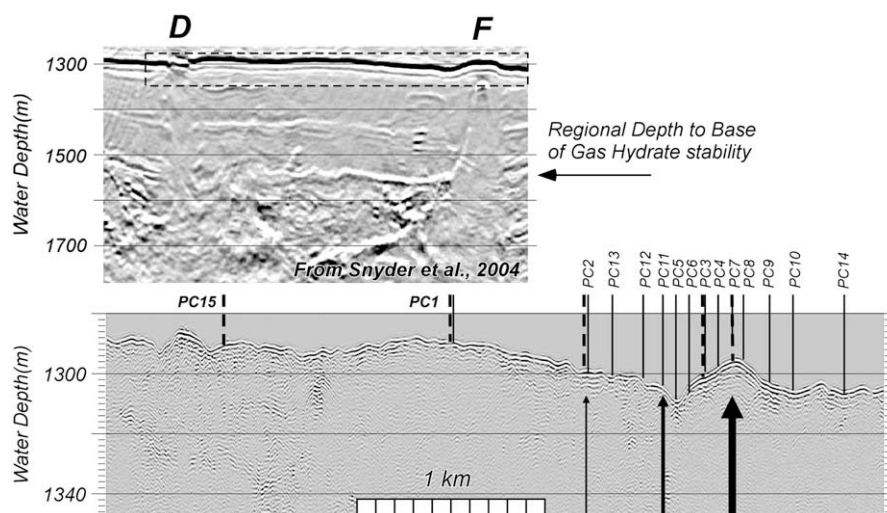


Fig. 2. Conventional USGS seismic profile from mound D to mound F (top profile) and DTAGS seismic profile from mound D to mound F (bottom profile after Wood et al., 2008). Vertical arrows on seismic profiles are sized relative to spatial variation in calculated vertical CH_4 flux. Piston core (PC) locations are identified on the DTAGS profile.

Sediment porosity was estimated using the method described by Hoehler et al. (2000). Frozen samples were thawed and allowed to equilibrate to room temperature overnight. Samples were then weighed, placed in a drying oven (50°C) overnight, and weighed again after drying to determine sediment–water content. The dried sediment samples were analyzed for percent organic carbon (%OC) using a Fisons EA 1108 with He carrier gas. Samples were treated with concentrated HCl vapor for 24 h prior to analysis to remove inorganic carbon.

2.3. Heat flow

Heat flow data were collected with a 3-m-long violin bow instrument with 11 thermistors arranged at 30 cm spacing in a 1-cm-diameter tube held in tension parallel to a solid steel strength member (Hyndman et al., 1979). The system measured both temperature gradient and thermal conductivity in situ. Sediment temperatures were calculated from the decay of the frictional heat caused by penetration of the instrument into the sediment. Thermal conductivity was determined from the decay of a calibrated thermal pulse applied after a preset period of time (Villinger and Davis, 1987).

2.4. Data evaluation

The SMT was chosen as the depth where minimum CH_4 and SO_4^{2-} concentrations converge plus half the depth to the next whole round section. For cores where vertical SO_4^{2-} profiles did not reach the limits of detection, the SMT was estimated by linear extrapolation of the SO_4^{2-} concentration vs. depth profile. While the depth of the SMT provides qualitative prediction of vertical CH_4 flux, quantitative estimates can be calculated from regression analysis of sediment porewater SO_4^{2-} profiles. Assuming steady-state conditions, SO_4^{2-} diffusion rates can be calculated from the linear fit to the SO_4^{2-} concentration gradient according to Fick's first law (Bernier, 1964, 1980):

$$J = -\phi D_s \frac{dc}{dx} \quad (1)$$

where J represents the SO_4^{2-} flux ($\text{mmol m}^{-2} \text{a}^{-1}$), ϕ is the sediment porosity, D_s is the diffusion coefficient, c is the range in SO_4^{2-}

concentration, and x is the range in depth for the linear section of the SO_4^{2-} porewater profile. D_s in Eq. (1) is given by:

$$D_s = \frac{D_0}{1 + n(1 - \phi)}, \quad (2)$$

where D_0 is assumed to be $8.7 \times 10^{-5} \text{ cm}^2 \text{ s}^{-1}$ (Iversen and Jørgensen, 1993), and $n = 3$ was adopted for the clay–silt sediments in this region. A 1:1 ratio of SR to CH_4 oxidation is typically present during AOM (Borowski et al., 1996). Therefore, SO_4^{2-} diffusion rates associated with AOM can be used for geospatial description of CH_4 flux on the scale of seismic and heat flow analysis. Data presented throughout the manuscript references downward SO_4^{2-} diffusion as negative (into the sediments) and upward CH_4 flux as positive (out of the sediments). In sediment cores with concave up porewater SO_4^{2-} profiles, linear portions of the SO_4^{2-} profile below the apparent mixing depth were selected for calculation of the SO_4^{2-} diffusion rate (Bernier, 1978).

3. Results

Porewater data were grouped into three categories based upon geochemical profiles and geographic position relative to mound F (Fig. 2): (1) off the mound (Fig. 3; cores 1, 2, 10, and 12–14); (2) top of mound (Fig. 4; cores 3, 4, and 6–8); and (3) base of mound (Fig. 5; cores 5, 9, 11, and 15). This grouping is intended to simplify the presentation of porewater profiles by spatially referencing cores to the mound, but is not intended to define the spatial extent of the influence of the mound or other geologic features or biogeochemical processes. The spatial distribution of the core sites is referenced to core 15, which was the most distant core from mound F.

Headspace CH_4 concentrations in all core sections ranged from $0.18 \mu\text{M}$ to 20.0 mM (Figs. 3–5). Top of mound headspace CH_4 concentrations tended to be high throughout the cores with values ranging between 1.74 and 13.9 mM (Fig. 4). Headspace CH_4 concentrations off the mound and at the base of the mound were below detection or at low concentrations in the surface sediments and generally increased from the SMT to the base of cores (Figs. 3 and 5).

Porewater sulfate concentrations ranged from 28.5 mM (seawater concentration) down to the limits of detection (LOD, 0.1 mM) (Figs. 3–5). Vertical porewater SO_4^{2-} profiles in cores collected off the mound or at the base of the mound generally decreased with

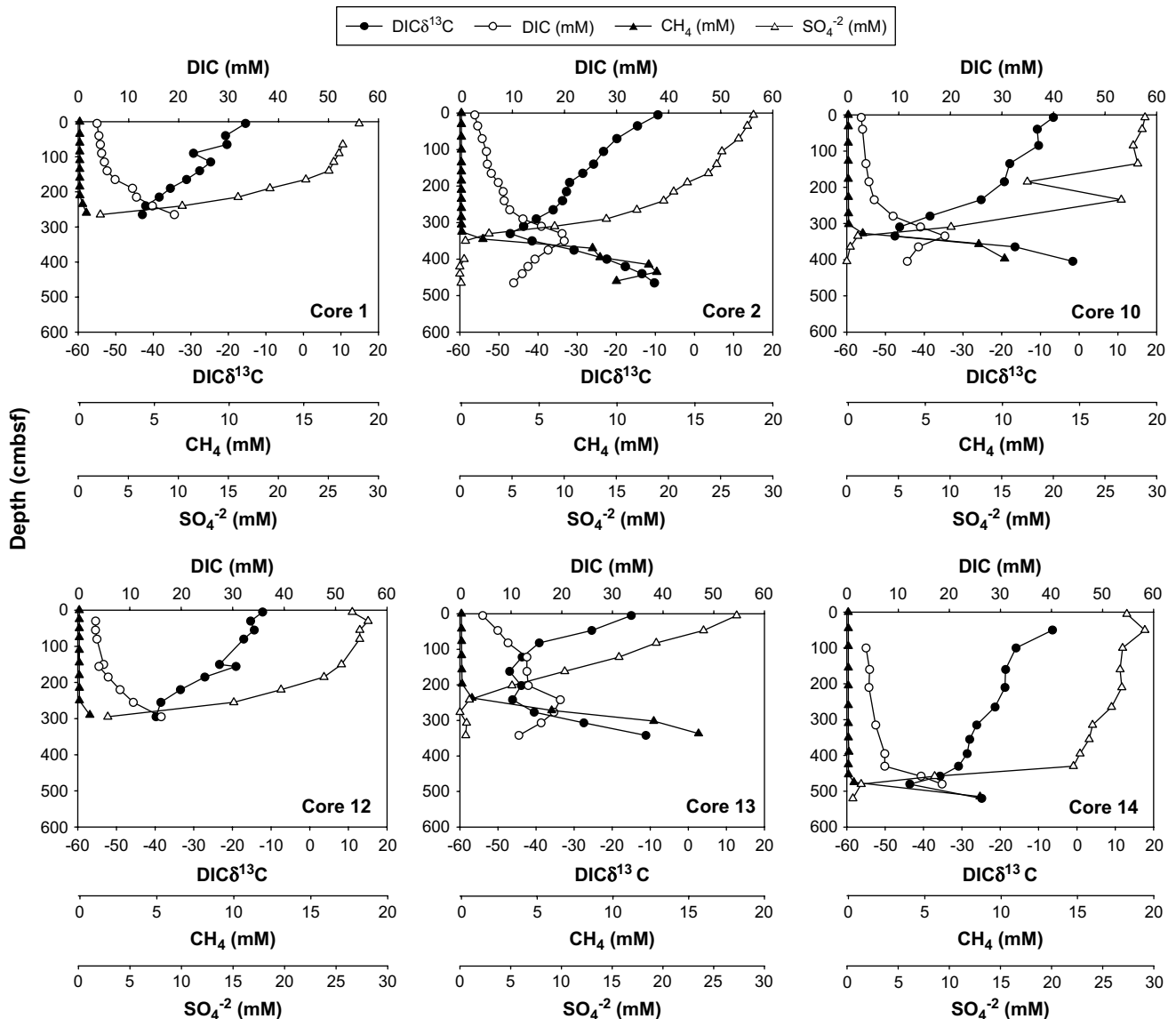


Fig. 3. Depth profiles of porewater parameters including CH_4 , SO_4^{2-} , DIC concentrations and the $\delta^{13}\text{C}$ -DIC for cores taken off the mound.

depth from the sediment–water interface to a minimum concentration used to predict the SMT (Figs. 3 and 5). Samples from the top of the mound contained little (<13 mM) or no SO_4^{2-} (<0.1 mM) (Fig. 4).

Porewater DIC concentrations ranged between 2.6 mM at the sediment–water interface in core 5 and 20.0 mM at the base of core 2 (Figs. 3–5). Generally, the highest DIC concentrations were observed in the vicinity of the SMT in off mound and base of the mound cores (Figs. 3 and 5). Porewater DIC concentrations in base of mound and top of mound cores had lower maximum values than off-mound cores (Figs. 4 and 5). On the mound porewater DIC concentrations were highest (average 10.2 mM) at depths above 100 cmbsf (Fig. 4).

Porewater DIC $\delta^{13}\text{C}$ ranged from -54.9‰ to 10.8‰ in all samples (Figs. 3–5). In off-mound core samples, DIC $\delta^{13}\text{C}$ averaged -27.2‰ (Fig. 3). In samples collected below 100 cmbsf, DIC $\delta^{13}\text{C}$ averaged -30.6‰ . In samples collected above 100 cmbsf, DIC $\delta^{13}\text{C}$ averaged -18.1‰ . For cores on the mound, DIC $\delta^{13}\text{C}$ averaged -5.5‰ with ^{13}C -depleted DIC (average -24.9‰) in samples collected above 100 cmbsf (Fig. 4). Generally, DIC on the mound samples was ^{13}C -enriched below 100 cmbsf (average 0.6‰). Porewater DIC $\delta^{13}\text{C}$

averaged -23.5‰ in cores taken at the base of the mound (Fig. 5). Compared to samples taken off mound and on top of the mound, there was not a large range in DIC $\delta^{13}\text{C}$ values from surface to bottom of the cores for the base of mound cores. Porewater DIC $\delta^{13}\text{C}$ averaged -20.8‰ above 100 cmbsf and -24.6‰ below 100 cmbsf in those cores.

Sediment porewater Cl^- concentrations ranged from 535.0 to 982.8 mM (Fig. 6A). Most off the mound cores had vertical porewater Cl^- concentrations near background seawater (560 mM). Cores 10 and 13 off the mound and core 5 from the base of the mound showed slightly elevated porewater Cl^- concentrations, greater than 600 mM, in the deeper sections. Cores 8 and 11 from the base of the mound showed a trend of increasing Cl^- concentration from near seawater at the sediment–water interface up to as high as 902.5 mM in the deepest subsample. The highest porewater Cl^- concentrations were observed on the mound in cores 3, 4, 6, and 7, with a range of 607.7–982.8 mM. The porewater Cl^- concentration measured in core 7 was as high as 956.5 mM near the sediment–water interface.

The spatial variations in estimated SMT depths and SO_4^{2-} diffusion rates are shown in Fig. 7. The SMT depths were estimated to be

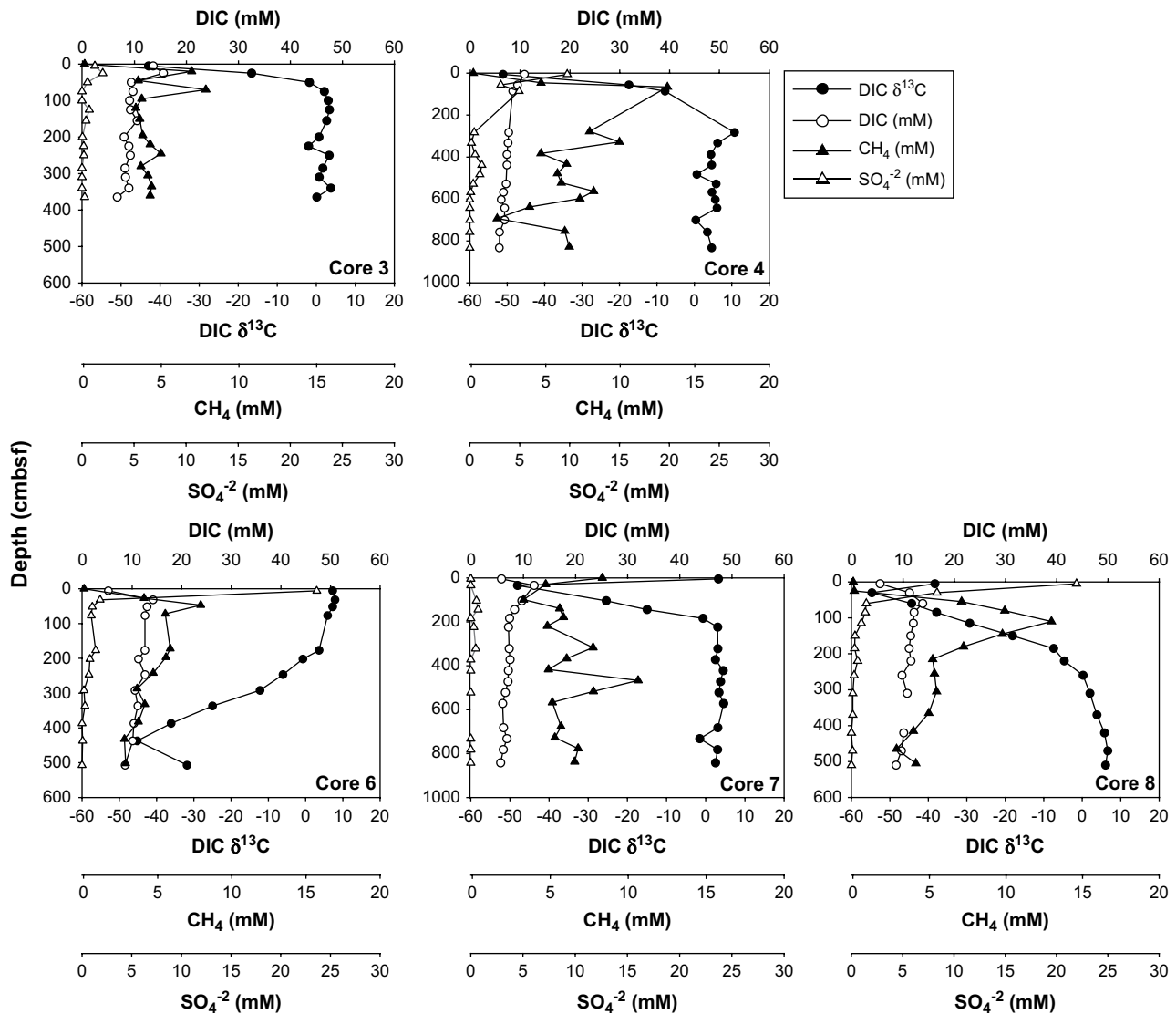


Fig. 4. Depth profiles of porewater parameters including CH_4 , SO_4^{2-} , DIC concentrations and the $\delta^{13}\text{C}$ -DIC for cores taken on the mound.

45 and 59 cmbsf for cores 6 and 8, respectively. Cores 3, 4 and 7 had high CH_4 concentrations and depleted SO_4^{2-} at shallow depths, suggesting that vertical CH_4 flux exceeded downward SO_4^{2-} diffusion. Deeper SMTs were observed in cores transitioning off mound F (cores 1, 2, 5, and, 9–15), with SMT depths ranging from 288 to 504 cmbsf (average 361 cmbsf). In cores near the base of mound F (cores 5, 9, 11, 15) the SMT ranged from 45 to 247 cmbsf (average 110 cmbsf).

Sulfate diffusion rates were estimated for cores where porewater SO_4^{2-} profiles appeared linear (cores 5, 6, 8, 9, 11, and 13). Diffusion rates were also estimated from the deeper linear portion of porewater SO_4^{2-} profiles approaching the SMT in cores where bioturbation in shallow sediment could have resulted in concave up profiles (cores 1, 12, and 15). Estimates of SO_4^{2-} diffusion rates were not made for the non-linear profiles found in cores 2, 10, and 14. Estimated SO_4^{2-} diffusion rates generally followed the variations in the SMT depth (Fig. 7). Sulfate diffusion rates ranged from -20.4 to $-249.1 \text{ mmol SO}_4^{2-} \text{ m}^{-2} \text{ a}^{-1}$ with minimum values off the mound. Off the mound SO_4^{2-} diffusion averaged $-54.7 \text{ mmol SO}_4^{2-} \text{ m}^{-2} \text{ a}^{-1}$ (range -20.4 to $-93.5 \text{ mmol SO}_4^{2-} \text{ m}^{-2} \text{ a}^{-1}$). Sulfate diffusion in cores from the base of the mound ranged from -44.5 to $-125.8 \text{ mmol SO}_4^{2-} \text{ m}^{-2} \text{ a}^{-1}$ (average $-75.8 \text{ mmol SO}_4^{2-} \text{ m}^{-2} \text{ a}^{-1}$).

The porewater SO_4^{2-} profiles found in cores 6 and 8 (top of mound) suggest diffusive flux of -249.1 and $-167.3 \text{ mmol SO}_4^{2-} \text{ m}^{-2} \text{ a}^{-1}$, respectively. In close proximity, a slight SO_4^{2-} concentration gradient in core 7 on the mound allows for an estimate of $-2.57 \text{ mmol SO}_4^{2-} \text{ m}^{-2} \text{ a}^{-1}$. Core 4 had varied and depleted shallow SO_4^{2-} concentrations, and a linear profile could not be used to infer diffusion rates. The SO_4^{2-} concentrations through core 3 were near the LOD.

4. Discussion

4.1. Porewater SO_4^{2-} profiles, estimated SO_4^{2-} diffusion rates, and headspace CH_4 measurements

The SO_4^{2-} diffusion rates estimated for Atwater Valley (-20.4 to $-249.1 \text{ mmol m}^{-2} \text{ a}^{-1}$) in this study are similar to values from studies in other deep marine regions that have been surveyed for hydrate deposits (Niewöhner et al., 1998; Dickens, 2001; Hensen et al., 2003; Treude et al., 2005; Coffin et al., 2006a). In sediments 5480 m deep off the coast of Uruguay, SO_4^{2-} diffusion rates ranged from -6.3 to $-162 \text{ mmol m}^{-2} \text{ a}^{-1}$ (Hensen et al., 2003). Off the western coast of Africa, in an area with seafloor depth ranging from 1312 to 2060 m SO_4^{2-} diffusion rates range from -21.5 to

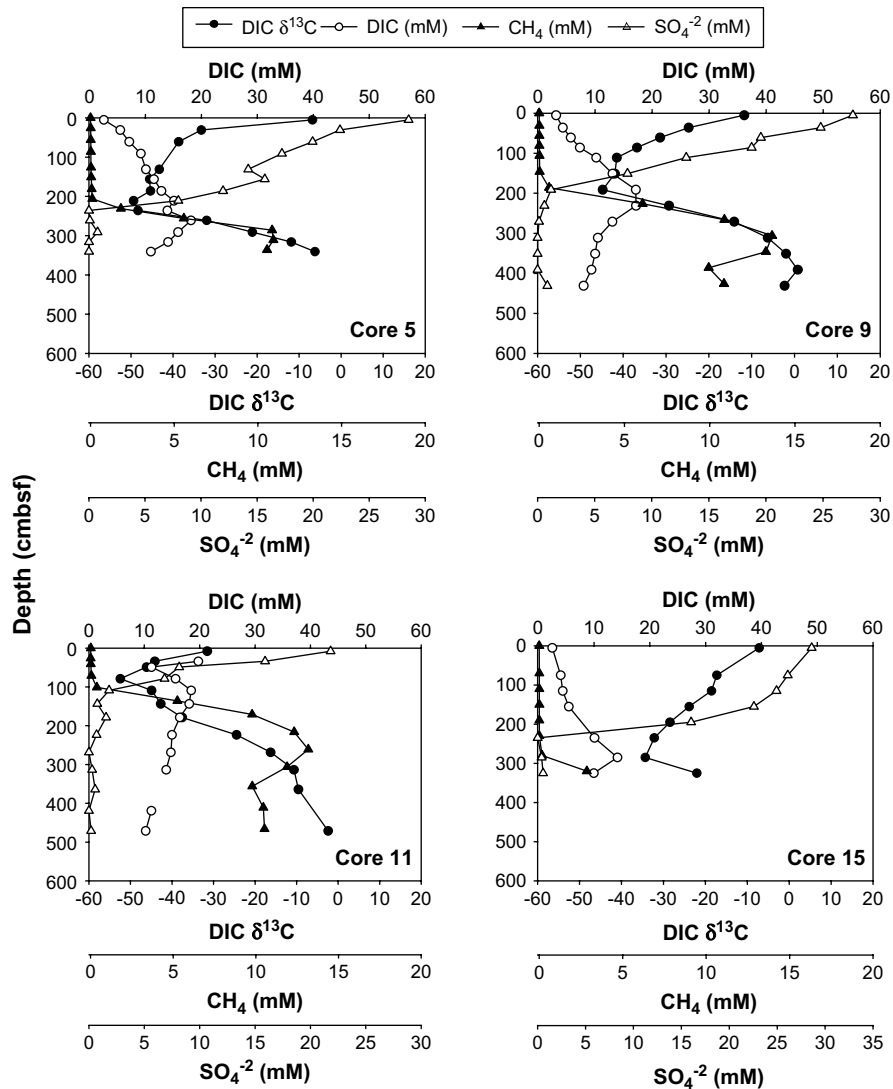


Fig. 5. Depth profiles of porewater parameters including CH_4 , SO_4^{2-} , DIC concentrations and the $\delta^{13}\text{C}$ -DIC for cores taken at the base of the mound.

$-61.5 \text{ mmol m}^{-2} \text{ a}^{-1}$ (Niewöhner et al., 1998). Sulfate diffusion rates along the mid to southern Chilean margin ranged between -22.9 and $-362.0 \text{ mmol m}^{-2} \text{ a}^{-1}$ (Treude et al., 2005; Coffin et al., 2006a). Substantially, lower diffusion rates, -7.2 to $-7.9 \text{ mmol m}^{-2} \text{ a}^{-1}$, were measured on Blake Ridge (Dickens, 2001). The shallow SMT and higher vertical sulfate diffusion rates measured through Atwater Valley could be an indication of vertical CH_4 fluxes from deep sediment hydrate deposits.

Our study showed large variations in porewater SO_4^{2-} profiles, estimated SO_4^{2-} diffusion rates, and SMT depths across a relatively short 3.5 km transect. The shallow SMT depths and high estimated SO_4^{2-} diffusion rates observed in cores 6 and 8, coupled with the high headspace CH_4 concentrations (averaging $5.6 \pm 2.5 \text{ mM}$) and depleted porewater SO_4^{2-} concentrations found in cores 3, 4, and 7, suggest that high CH_4 flux occurs on the mound (Fig. 7). The porewater headspace CH_4 and SO_4^{2-} profiles in other sediment cores (Figs. 3–5 and 7) indicate potential for a wide range of CH_4 flux and SO_4^{2-} diffusion rates, with more rapid rates estimated at the base of the mound (average $-75.8 \text{ mmol SO}_4^{2-} \text{ m}^{-2} \text{ a}^{-1}$) and lower flux off the mound (average $-54.7 \text{ mmol SO}_4^{2-} \text{ m}^{-2} \text{ a}^{-1}$). Data from the transect as a whole suggest that both steady-state and non-steady-state CH_4 fluxes are occurring both on and off the mound.

Application of shallow sediment SMT data to predict vertical diffusion of deep sediment CH_4 requires linear SO_4^{2-} and CH_4 profiles or understanding of the parameters that result in non-steady-state profiles. The porewater SO_4^{2-} and headspace CH_4 profiles in this study were linear, concave up and concave down, and irregular (kinked or S-shaped) (Figs. 3–5). Of all the off-mound cores, only core 13 exhibited what appeared to be a linear, steady-state diffusive porewater SO_4^{2-} and headspace CH_4 profile. More linear profiles were observed on and at the base of the mound. High, variable headspace CH_4 concentrations were measured at shallow depths in cores taken on the mound with elevated CH_4 concentration observed up to the sediment–water column interface in core 7. The variable CH_4 concentrations found in cores 3, 4, and 7 on the mound may be related to non-steady-state fluxes or fluid advection.

Rates of SO_4^{2-} diffusion through shallow sediments are affected by biotic and abiotic factors (Berner, 1978; Joye et al., 2004; Dickens, 2001). These factors include changes in sediment stability, horizontal migration of porewater resulting from rapid vertical fluid fluxes, variations in vertical CH_4 fluxes, deep sediment petroleum seeps, bioturbation, and bioirrigation (Fossing et al., 2000; Hensen et al., 2003; Aharon and Fu, 2003; Joye et al., 2004; Coffin et al., 2006a). Over a large spatial scale ($\sim 100 \text{ km}$)

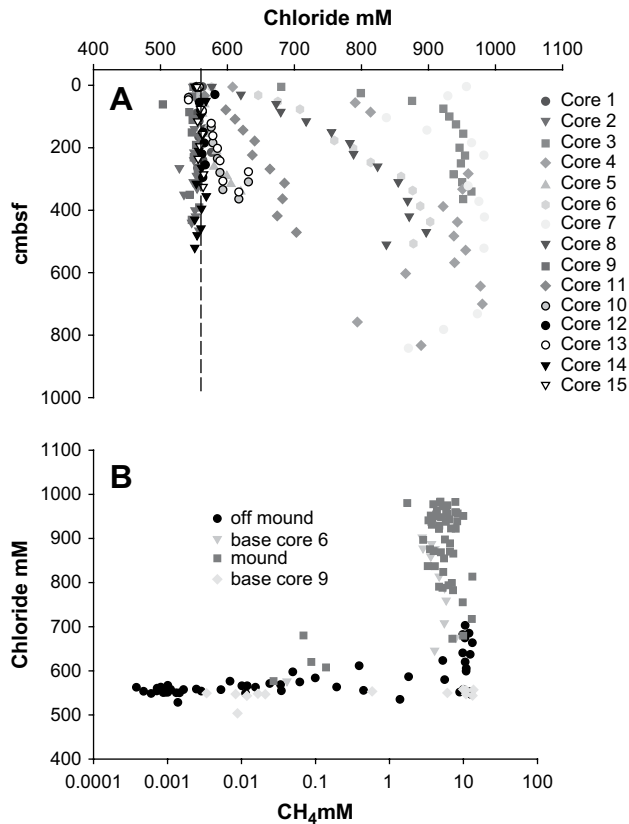


Fig. 6. Depth profiles of porewater chloride concentration. Dashed vertical line references background seawater Cl⁻ concentration of 560 mM (A). Chloride data plotted against CH₄ concentration (B).

off the coast of Argentina, concave up, concave down, linear, S-typed and kinked SO₄²⁻ profiles were attributed to sedimentary slides and variations in vertical methane fluxes (Hensen et al., 2003). Over the small spatial scale in our study at Atwater Valley (3.5 km) we postulate that the variation in observed SO₄²⁻ profiles results from differences in the relative contribution of fluid advection to the CH₄ flux.

The porewater SO₄²⁻ profiles observed during this study may also be partially a result of SR not coupled to AOM but instead related to organoclastic SR in shallow section of the cores (Iversen and Jørgensen, 1985). The concave down profiles observed in cores 5 and 11 suggest active organoclastic SR (Berner, 1978, 1980; Westrich and Berner, 1984). The concave up SO₄²⁻ profiles observed in cores off and at the base of the mound could result from combined bioturbation and organoclastic SR in the shallow sediments (Hensen et al., 2003). Sulfate reduction not coupled to AOM has been observed in other studies in the Gulf of Mexico where sediments are located over thermogenic gas and petroleum seeps (Whelan et al., 2005; Joye et al., 2004; Aharon and Fu, 2003). In these locations SR occurs through cycling of petroleum based hydrocarbons rather than CH₄, resulting in non-steady-state SO₄²⁻ profiles (Joye et al., 2004). In our study in Atwater Valley, δ¹³C data indicate that CH₄ is of biogenic origin (Coffin et al., 2006b), and other, petroleum-related hydrocarbons were not present in significant concentrations in the samples analyzed. Sediment organic carbon δ¹³C off the mound (Coffin et al., 2005a) is similar to values for marine phytoplankton (-22‰) supporting organoclastic SR in shallow sediments with slower CH₄ diffusion.

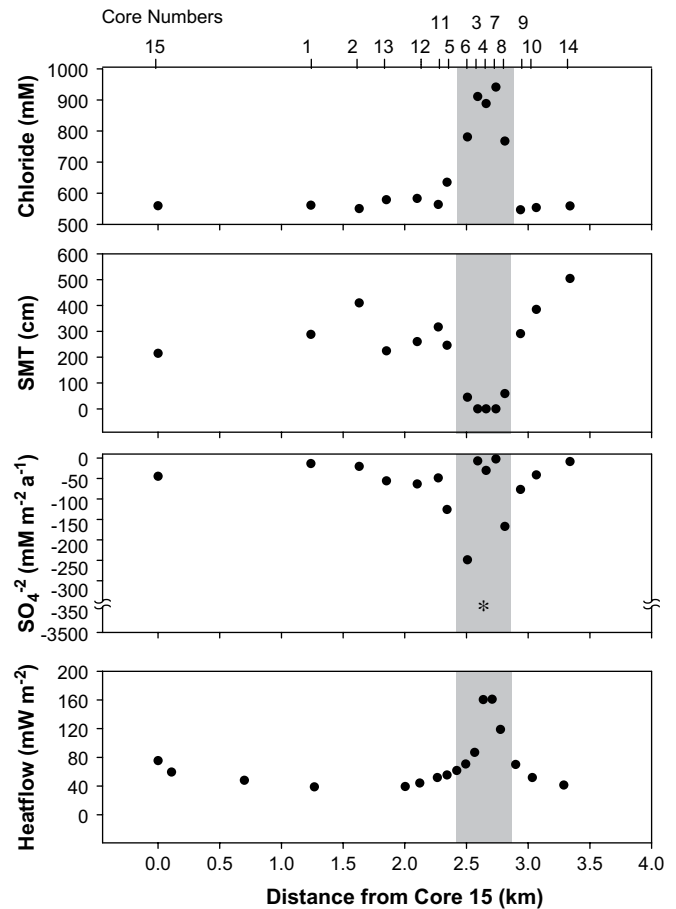


Fig. 7. Summary of vertical SO₄²⁻ diffusion rates and SMT depths compared to heat flow and porewater Cl⁻ concentration for coring stations taken along the DTAGS line from mound D to mound F. The estimated upper limit for SO₄²⁻ diffusion on the mound is indicated by the symbol (*). For spatial comparison core locations are referenced in distance away from core 15, located furthest off of mound F. Core numbers are listed in the top panel. For relative two dimensional positioning of the cores refer to Fig. 1.

4.2. Evidence for fluid advection and methane flux on the mound

The progressive decrease in SMT depth toward the apex of the mound and associated increases in estimated SO₄²⁻ diffusion rates and measured high concentrations of CH₄ were consistent with shoaling of a BSR beneath the mound and a deeper, flat BSR away from the mound (Figs. 2 and 7). Coincident heat flow measurements yielded 40–50 mW m⁻² at the locations of cores 1 and 2 off the mound to 160 mW m⁻² near cores 3, 4, and 7 on mound F (Fig. 7). In those mound F cores, the estimated vertical SO₄²⁻ diffusion rate was lowest (up to -2.57 mmol SO₄²⁻ m⁻² a⁻¹) or could not be estimated due to the absence of measurable SO₄²⁻ (Figs. 4 and 7). This could result from porewater advection out of the sediments exceeding downward SO₄²⁻ diffusion and/or rapid SO₄²⁻ reduction (organoclastic SR or AOM) occurring at or near the sediment–water column interface. Low seismic backscatter and sidescan sonar, multi-beam bathymetry, and near bottom photography by Hart et al. (2008) indicate rapid to moderate fluid flux at mound F, supporting our interpretation of advective CH₄ profiles on the mound.

The SO₄²⁻ profiles in this study are consistent with other studies in the Gulf of Mexico that indicate shoaling of the SMT over seeps. On Garden Bank (GB425) and Mississippi Canyon (MC852/853) mud mounds have been described to contain migrating fluids as a result of over pressured sediments above salt structures. At these

locations active fluid migration is interpreted by the observation of distinct barite precipitation and dissolution profiles that occur in regions of active advection with a shoaling of the SMT (Castellini et al., 2006). Elevated Cl^- and CH_4 concentrations that we measured in cores on the mound and at the base of the mound suggest the existence of similar patterns of fluid migration (Fig. 6).

Although vertical flux rates could not be estimated from SO_4^{2-} and CH_4 profiles in cores 3, 4 and 7 on the mound, DIC $\delta^{13}\text{C}$ data provide evidence for AOM at this location. The CH_4 $\delta^{13}\text{C}$ observed in the study region is approximately -71% (Coffin et al., 2006b; Claypool, 2006) and would show a traceable signature in the $\delta^{13}\text{C}$ DIC associated with active CH_4 oxidation to DIC. Recent studies indicate that $\delta^{13}\text{C}$ for organic matter in sediment on the northern Texas–Louisiana Shelf generally ranges from -23% to -20% (Gordon and Goñi, 2004; Goñi et al., 1998). While there is a large range in the sediment porewater DIC $\delta^{13}\text{C}$ data (-54.7% to 10.8%) in this study, DIC was consistently ^{13}C -depleted (more negative; $\sim -50\%$ to -30%) in porewaters measured through the SMT in cores taken at the base and off the mound. In cores 3, 4 and 7 (top of the mound), this same trend in ^{13}C -depleted DIC was observed above 100 cmbsf (Fig. 4) and, when coupled with high CH_4 concentrations (averaged 5.1 mM), suggests active AOM.

Approximation of the SO_4^{2-} diffusion rates at the sediment–water column interface can be applied to estimate maximum vertical CH_4 flux for cores 3 and 7 located on the mound. Here, SO_4^{2-} concentration in seawater is predicted to be similar to that measured in off-mound shallow sediments (27.7 mM). Porewaters from above 5 cmbsf in cores 3 and 7 had SO_4^{2-} concentrations of 1.2 mM and 0.0 mM, respectively. Assuming all porewater SO_4^{2-} is consumed through AOM in the upper 5 cm results in an estimate for diffusion of $-3250 \text{ mmol SO}_4^{2-} \text{ m}^{-2} \text{ a}^{-1}$ (Fig. 7). This upper limit diffusion rate is approximately an order of magnitude greater than diffusion rates calculated at the base and off the mound. Methane advection rates have been estimated to be as high as $8680 \text{ CH}_4 \text{ mmol m}^{-2} \text{ a}^{-1}$ on Hydrate Ridge (Luff and Wallmann, 2003). Thus if one assumes SR coupled to AOM is consuming CH_4 at a 1:1 ratio to SO_4^{2-} , then the upper limit for SO_4^{2-} diffusion estimated at cores 3 and 7 suggests high CH_4 flux is occurring on mound F (Fig. 7). This conclusion is consistent with elevated heat flow (160 mW m^{-2}) on the mound near cores 3, 4 and 7.

Reports from other studies on the Texas–Louisiana Shelf show a strong contrast with the SO_4^{2-} and CH_4 cycling inferred in Atwater Valley. Green Canyon sites GC234 and GC285 are located in an area characterized by thermogenic gas and petroleum seeps (Joye et al., 2004). Average AOM rates are $1022 \text{ mmol CH}_4 \text{ m}^{-2} \text{ a}^{-1}$, and SR rates coupled with oxidation of seep petroleum or higher molecular weight gases averaged $19,710 \text{ SO}_4^{2-} \text{ mmol m}^{-2} \text{ a}^{-1}$ (Joye et al., 2004). A combination of these two cycles in SR is estimated to be $\sim 21,000 \text{ SO}_4^{2-} \text{ mmol m}^{-2} \text{ a}^{-1}$. The Green Canyon sediments have on average 2–6% (Joye et al., 2004) organic carbon, much higher than 0.6–0.7% we measure in Atwater Valley cores 2 and 7. At GC and other sites with advection of deep petroleum and higher molecular weight carbon gases, SR independent of AOM is the primary pathway for the consumption of SO_4^{2-} . In Atwater Valley the low organic carbon content of the sediments suggests AOM is a large fraction of total SR. Similar results are presented for Keathley Canyon where AOM was found to be a dominant cycle in the SR (Pohlman et al., 2008).

4.3. Hydrate stability and elevated porewater chloride

Elevated porewater Cl^- was observed above the seawater background in a distinct spatial distribution between cores off the mound, at the base, and on the mound (Figs. 6b and 7). Typically sediment porewaters with Cl^- concentrations below that of seawater (560 mM) are indicative of hydrate dissociation (Ussler and

Paull, 2001; Paull et al., 2005). Among the 15 cores analyzed (Fig. 6A), porewater freshening was only observed in one sample taken from core 9, located near the visual observation of the mud flow (Hart et al., 2008).

Ruppel et al. (2005) report high salinity porewaters in advective fluid flow regimes in other parts of the northern Gulf of Mexico. Experiments have shown that increases in porewater salinity result in decreased stability of hydrates (de Roo et al., 1983). In our study, high Cl^- concentrations frequently coincided with high dissolved CH_4 concentrations, suggesting increased hydrate instability from locally elevated salt concentrations (Fig. 6b). The trend at Atwater Valley of high Cl^- concentrations and elevated CH_4 concentrations on the mound transitioning to intermediate CH_4 and Cl^- concentrations at the base of the mound and then to background (seawater) Cl^- concentrations and low CH_4 away from the mound would be consistent with a decrease in the thickness of the hydrate stability zone approaching the mound. High porewater Cl^- concentrations measured in this study and in the porewaters over other gas hydrate mounds are consistent with reports of abundant salt intrusions and diapirs in the northern Gulf of Mexico (Weimer and Buffler, 1992; Grando and McClay, 2004; Stewart, 2006). Other elements have also been related to the vertical diffusion of Cl^- originating from salt diapirs in Atwater Valley. In a series of deep coring and wells drilled at this site, concentrations of Br, I, and Ba^{+2} were found to be high on mound (core 3) and lower off the mound (core 1) (Claypool, 2006).

At mounds located in several northern Gulf of Mexico locations, gas hydrates containing gases of either biogenic or thermogenic origin were inferred to be largely unstable in shallow sediments due to measured high salinities in porewaters and elevated temperatures (Ruppel et al., 2005). This inference is supported by the detection of high salinity porewaters at all mound sites sampled in a jumbo piston coring study across a broad swath of the northern Gulf of Mexico by Paull et al. (2005). At the Atwater Valley mounds, porewater gas composition and $\delta^{13}\text{C}$ values indicate a biogenic source of methane (Coffin et al., 2005a). Structure I hydrates, forming from biogenic CH_4 at our study site would be less stable than methane-dominated Structure II thermogenic hydrates when subjected to the same elevated salinity and heat conditions (Sloan, 1998; Ruppel et al., 2005; Lu and Matsumoto, 2005).

5. Conclusions

Methane and SO_4^{2-} measurements have been applied to provide estimates of SO_4^{2-} diffusion into sediments. These results can be used to estimate CH_4 fluxes and evaluate seismic data applied to deep sediment methane hydrate exploration. Because seismic surveys do not always provide a direct indication of the presence of gas and gas hydrate in sediments, models which incorporate measurements of SO_4^{2-} and CH_4 may improve the predictive capability of seismic detection of gas hydrates. As seismic detection remains the most practical tool for detecting possible locations for deep sediment drilling for gas hydrates, it is of vital importance to integrate this tool with geochemical data. However, non-steady-state processes frequently limit the quantitative prediction of CH_4 flux and estimation of deep sediment gas and gas hydrate.

In this study, variations in estimated sediment SMT depths and SO_4^{2-} diffusion rates are consistent with seismic profiles and the variation in measured heat flow data over short distances. Seismic profiles across the same locations showed a deep BSR off the mound with reflections shoaling toward the mound. Results suggest that variation in deep sediment CH_4 fluxes may be inferred based upon the depth of the SMT and the estimated rate of SO_4^{2-} diffusion into surface sediment. It is likely that salinity effects influence hydrate stability in this region, given the high Cl^- concentrations and elevated CH_4 concentrations in porewater samples

on the mound. Such information can aid in locating and predicting areas of hydrate instability as well as aid in understanding the meaning of seismic blanking zones. Seismic profiles, heat flow data, and geochemical data all suggest vertical fluid migration is occurring on the mound. Recently, efforts have been made to integrate diffusive and advective fluid flux estimates with calculations of CH₄ content and export from marine sediments (Hesse, 2003). Future research needs to focus on estimating the contribution of advective fluid migration to CH₄ flux in this region on large and small spatial scales.

At Atwater Valley non-steady-state SO₄²⁻ profiles appear to partially result from organoclastic SR in shallow sediments. Other factors which may influence non-steady-state profiles are fluid advection, variable CH₄ flux, bioturbation or shallow sediment slides. Determining the parameters that result in non-steady-state SO₄²⁻ profiles will allow more accurate estimates of SO₄²⁻ diffusion and CH₄ flux. Such estimates may contribute to predictions of the size and magnitude of gas hydrate deposits as well as CH₄ subsidy to the overlying water column.

Acknowledgements

J. Pohlman, then at NRL and VIMS, was responsible for the ship board laboratory operation that provided field porewater data. R. Downer was leader for all coring operations. We appreciate the support by the crew of the *R/V Gyre*. This research was supported by DoE/NETL, ONR and NRL.

References

- Aharon, P., Fu, B., 2000. Microbial sulfate reduction rates and sulfur and oxygen isotope fractionations at oil and gas seeps in deepwater Gulf of Mexico. *Geochim. Cosmochim. Acta* 64, 233–246.
- Aharon, P., Fu, B., 2003. Sulfur and oxygen isotopes of coeval sulfate–sulfide in pore fluids of cold seep sediments with sharp redox gradients. *Chem. Geol.* 195, 201–218.
- Berner, R.A., 1964. An idealized model of dissolved sulfate distribution in recent sediments. *Geochim. Cosmochim. Acta* 28, 1497–1503.
- Berner, R.A., 1978. Sulfate reduction and the rate of deposition of marine sediments. *Earth Planet. Sci. Lett.* 37, 492–498.
- Berner, R.A., 1980. *Early Diagenesis – A Theoretical Approach*. Princeton University Press.
- Boehme, S.E., Blair, N.E., Chanton, J.P., Martens, C.S., 1996. A mass balance of ¹³C and ¹²C in an organic-rich methane-producing marine sediment. *Geochim. Cosmo. Acta* 60, 3835–3848.
- Boetius, A., Ravensschlag, K., Schubert, C.J., Rickert, D., Widdel, F., Gieseke, A., Amann, R., Jørgensen, B.B., Witte, U., Pfannkuche, O., 2000. A marine microbial consortium apparently mediating anaerobic oxidation of methane. *Nature* 407, 623–626.
- Borowski, W.S., Paull, C.K., Ussler III, W., 1996. Marine porewater sulfate profiles indicate in situ methane flux from underlying gas hydrate. *Geology* 24, 655–658.
- Borowski, W.S., Paull, C.K., Ussler III, W., 1999. Global and local variations of interstitial sulfate gradients in the deep-water, continental margin sediments: sensitivity to underlying methane and gas hydrates. *Mar. Geol.* 159, 131–154.
- Castellini, D.G., Dickens, G.R., Snyder, G.T., Ruppel, C.D., 2006. Barium cycling in shallow sediments above active mud volcanoes in the Gulf of Mexico. *Chem. Geol.* 226, 1–30.
- Claypool, G.E. (Ed.), 2006. Cruise Report: The Gulf of Mexico Gas Hydrate Joint Industry Project, Covering the Cruise of the Drilling Vessel Uncle John, Mobile, Alabama to Galveston, Texas, Atwater Valley Blocks 13/14 and Keathley Canyon Blocks 151, 17 April to 22 May, 2005. Dept. of Energy, 196 pp. Available from: <http://www.netl.doe.gov/technologies/oil-gas/publications/Hydrates/reports/GOMJIPCruise05.pdf>.
- Coffin, R.B., Gardner, J., Pohlman, J.W., Downer, R.Z., Wood, W.T., 2005a. Methane hydrate exploration, Atwater Valley, Texas–Louisiana Shelf: Geophysical and geochemical profiles. Fourth Workshop of the International Committee on Gas Hydrates Research and Development. Victoria, British Columbia, Canada, May 9–11.
- Coffin, R.B., Gardner, J., Pohlman, J., Downer, R., Wood, W., 2006b. Methane Hydrate Exploration, Atwater Valley, Texas–Louisiana Shelf: Geophysical and Geochemical Profiles. US Naval Research Laboratory Technical Memorandum, NRL/MR/6110–06–9002.
- Coffin, R., Pohlman, J., Wood, W., Gardner, J., Plummer, R., Gettrust, J., 2005b. Geochemical evaluation of piston core porewater on Atwater Valley, Gulf of Mexico: variation in vertical methane gradients. *EOS, Trans. AGU* 86 (52) Abstract OS42A–03.
- Coffin, R.B., Pohlman, J.W., Gardner, J., Downer, R., Wood, W., Hamdan, L., Walker, S., Plummer, R., Gettrust, J., Diaz, J., 2006a. Methane hydrate exploration on the Mid Chilean coast: a geochemical and geophysical survey. *J. Pet. Sci. Eng.* 56, 32–41, doi:10.1016/j.petrol.2006.01.013.
- Cooper, A.K., Hart, P.E., 2003. High-resolution seismic-reflection investigation of the northern Gulf of Mexico gas hydrate stability zone. *Mar. Petr. Geol.* 19, 1275–1293.
- Dickens, G.R., 2001. Sulfate profiles and barium fronts in sediment on the Blake Ridge: present and past methane fluxes through a large gas hydrate reservoir. *Geochim. Cosmochim. Acta* 65, 529–543.
- Ellwood, B.B., Balsam, W.L., Roberts, H.H., 2006. Gulf of Mexico sediment sources and sediment transport trends from magnetic susceptibility measurements of surface samples. *Mar. Geol.* 230, 237–248.
- Fossing, H., Ferdelman, T.G., Berg, P., 2000. Sulfate reduction and methane oxidation in continental margin sediments influenced by irrigation (South-East Atlantic off Namibia). *Geochim. Cosmo. Acta* 64, 897–910.
- Goñi, M.A., Ruttenger, K.C., Eglinton, T.I., 1998. A reassessment of the sources and importance of land-derived organic matter in surface sediments from the Gulf of Mexico. *Geochim. Cosmo. Acta* 62, 3055–3075.
- Goodwin, R.H., Prior, D.B., 1989. Geometry and depositional sequences of the Mississippi Canyon, Gulf of Mexico. *J. Sed. Res.* 59, 318–329.
- Gordon, E.S., Goñi, M.A., 2004. Controls on the distribution and accumulation of terrigenous organic matter in sediments from the Mississippi and Atchafalaya river margin. *Mar. Chem.* 92, 331–352.
- Grando, G., McClay, K., 2004. Structural evolution of the Frampton growth fold system, Atwater Valley–Southern Green Canyon area, deep water Gulf of Mexico. *Mar. Pet. Geol.* 21, 889–910.
- Hart, P.E., Hutchinson, D.R., Gardner, J., Carney, R.S., Fornari, D., 2008. A photographic and acoustic transect across two deep-water seafloor mounds, Mississippi Canyon, northern Gulf of Mexico. *Mar. Petr. Geol.* 25, 969–976.
- Hensen, C., Zabel, M., Pfeifer, K., Schwenk, T., Kasten, S., Riedinger, N., Schulz, H.D., Boetius, A., 2003. Control of sulfate porewater profiles by sedimentary events and the significance of anaerobic oxidation of methane for the burial of sulfur in marine sediments. *Geochim. Cosmo. Acta* 67, 2631–2647.
- Hesse, R., 2003. Porewater anomalies of submarine gas-hydrate zones as tool to assess hydrate abundance and distribution in the subsurface. What have we learned in the past decade? *Earth-Sci. Rev.* 61, 149–179.
- Hoehler, T.M., Borowski, W.S., Alperin, M.J., Rodriguez, N.M., Paull, C.K., 2000. Model stable isotope and radiocarbon characterization of anaerobic methane oxidation in gas hydrate-bearing sediments of the Blake Ridge. *Proc. Ocean Drilling Prog., Sci. Results* 164, 79–85.
- Hutchinson, D.R., Hart, P.E., 2004. Cruise report for G1-03-GM USGS gas hydrates cruise, R/V Gyre, 1–14 May, 2003, northern Gulf of Mexico. U.S. Geological Survey Open File Report OF 03-474, 103 pp.
- Hutchinson, D.R., Hart, P.E., Ruppel, C.D., Snyder, F., Dugan, B., 2008. Seismic and thermal characterization of a bottom simulating reflection in the northern Gulf of Mexico. In: Collett, T.S., Johnson, A., Knapp, C., Boswell, R. (Eds.), *Natural Gas Hydrates: Energy Resources, Potential and Associated Geologic Hazards*. AAPG Special Publication.
- Hyndman, R.D., Davis, E.E., Wright, J.A., 1979. The measurement of marine geothermal heat flow by a multipenetration probe with digital acoustic telemetry and insitu thermal conductivity. *Mar. Geophys. Res.* 4, 181–205.
- Iversen, N., Jørgensen, B.B., 1985. Anaerobic methane oxidation rates at the sulphate–methane transition in marine sediments from Kattegat and Skagerrak (Denmark). *Limnol. Oceanogr.* 30, 944–955.
- Iversen, N., Jørgensen, B.B., 1993. Diffusion coefficients of sulfate and methane in marine sediments: influence of porosity. *Geochim. Cosmo. Acta* 57, 571–578.
- Joye, S.B., Boetius, A., Orcutt, B.N., Montoya, J.P., Schulz, H.N., Erickson, M.J., Lugo, S.K., 2004. The anaerobic oxidation of methane and sulfate reduction in sediments from Gulf of Mexico cold seeps. *Chem. Geol.* 205, 219–238.
- Kvenvolden, K.A., 2000. Natural gas hydrate: introduction and history of discovery. In: Max, M.D. (Ed.), *Natural Gas Hydrate in Oceanic and Permafrost Environments*. Kluwer, Netherlands, pp. 9–16.
- Lu, H., Matsumoto, R., 2005. Experimental studies on the possible influences of composition changes of porewater on the stability conditions of methane hydrate in marine sediments. *Mar. Chem.* 93, 149–157.
- Luff, R., Wallmann, K., 2003. Fluid flow, methane fluxes, carbonate precipitation and biogeochemical turnover in gas hydrate-bearing sediments at Hydrate Ridge, Cascadia Margin: numerical modeling and mass balances. *Geochim. Cosmochim. Acta* 67, 3403–3421.
- Milkov, A.V., Sassen, R., 2001. Estimate of gas hydrate resource, northwestern Gulf of Mexico continental slope. *Mar. Geol.* 179, 71–83.
- Milkov, A.V., Sassen, R., 2002. Economic geology of offshore gas hydrate accumulations and provinces. *Mar. Petr. Geol.* 19, 1–11.
- Milkov, A.V., Claypool, G.E., Lee, Y.J., Xu, W.Y., Dickens, G.R., Borowski, W.S., 2003. In situ methane concentrations, at Hydrate Ridge, offshore Oregon: new constraints on the global gas hydrate inventory from an active margin. *Geology* 31, 833–836.
- Milkov, A.V., Sassen, R., 2003. Preliminary assessment of resources and economic potential of individual gas hydrate accumulations in the Gulf of Mexico continental slope. *Mar. Petr. Geol.* 20, 111–128.
- Niewöhner, C., Hensen, C., Kasten, S., Zabel, M., Schulz, H.D., 1998. Deep sulfate reduction completely mediated by anaerobic methane oxidation in sediments of the upwelling area off Namibia. *Geochim. Cosmo. Acta* 62, 455–464.
- Orphan, V.J., Hinrichs, K.U., Ussler III, W., Paull, C.K., Taylor, L.T., Sylva, S.P., Hayes, J.M., Delong, E.F., 2001. Comparative analysis of methane-oxidizing archaea and

- sulfate-reducing bacteria in anoxic marine sediments. *Appl. Environ. Microbiol.* 67, 1922–1934.
- Pancost, R.D., Damste, J.S.S., de Lint, S., van der Maarel, M.J.E.C., Gottschal, J.C., Medinaut Shipboard Scientific Party, 2000. Biomarker evidence for widespread anaerobic methane oxidation in Mediterranean sediments by a consortium of methanogenic archaea and bacteria. *Appl. Environ. Microbiol.* 66, 1126–1132.
- Paull, C.K., Matsumoto, R., Wallace, P.J., et al., 1996. *Proc. Ocean Drilling Prog.: Initial Reports 164*. Ocean Drilling Program, College Station, Texas, doi:10.2973/odp.proc.ir.164.1996.
- Paull, C.K., Ussler, W., Lorenson, T.D., Winters, W., Dougherty, J.A., 2005. Geochemical constraints on the distribution of gas hydrates in the Gulf of Mexico. *Geo-Mar. Lett.* 25, 273–280.
- Pohlman, J.W., Ruppel, C., Hutchinson, D., Downer, R.Z., Coffin, R.B., 2008. Assessing sulfate reduction and methane cycling in a high salinity pore water system in the northern Gulf of Mexico. *Mar. Petr. Geol.* 25, 942–951.
- Reeburgh, W.S., 1967. An improved interstitial water sampler. *Limnol. Oceanogr.* 12, 163–165.
- Riedinger, N., Kasten, S., Groger, J., Franke, C., Pfeifer, K., 2006. Active and buried authigenic barite fronts in sediments from the Eastern Cape Basin. *Earth Planet. Sci. Lett.* 241, 876–887.
- de Roo, J.L., Peters, C.J., Lichtenthaler, R.N., Diepen, G.A.M., 1983. Occurrence of methane hydrate in saturated and unsaturated solutions of sodium chloride and water in dependence of temperature and pressure. *AIChE J.* 29, 651–657.
- Ruppel, C., Dickens, G.R., Castellini, D.G., Gilhooly, W., Lizarralde, D., 2005. Heat and salt inhibition of gas hydrate formation in the northern Gulf of Mexico. *Geophys. Res. Lett.* 32, L04604, doi:10.1029/2004GL021909.
- Sloan, E.D., 1998. *Clathrate Hydrates of Natural Gases*, second ed. Marcel Dekker, New York, 705 pp.
- Snyder, F.F.C., Muller, L.K., Dutta, N., Hutchinson, D.R., Hart, P.E., Lee, M.W., Dugan, B., Ruppel, C., Wood, W.T., Coffin, R., Evans, R., Jones, E.H., 2004. Seismic analysis and characterization of gas hydrates in the Northern Deepwater Gulf of Mexico. Available from: AAPG Bull. 88 (Suppl. 13) Available from: <http://www.search-anddiscovery.com/documents/abstracts/annual2004/Dallas/Snyder.htm>.
- Stewart, S.A., 2006. Implications of passive salt diapir kinematics for reservoir segmentation and radial and concentric faults. *Mar. Petr. Geol.* 23, 843–853.
- Torres, M.E., McManus, J., Hammond, D.E., De Angelis, M.A., Heeschen, K.U., Colbert, S.L., Tryon, M.D., Brown, K.M., Suess, E., 2002. Fluid and chemical fluxes in and out of sediments hosting methane hydrate deposits on Hydrate Ridge, OR, I: Hydrological provinces. *Earth Planet. Sci. Lett.* 201, 525–540.
- Treude, T., Niggemann, J., Kallmeyer, J., Wintersteller, P., Schubert, C.J., Boetius, A., Jørgensen, B.B., 2005. Anaerobic oxidation of methane and sulfate reduction along the Chilean continental margin. *Geochim. Cosmochim. Acta* 69, 2767–2779.
- Ussler III, W., Paull, C.K., 2001. Ion exclusion associated with marine gas-hydrate deposits. In: Paull, C.K., Dillon, W.P. (Eds.), *Natural Gas Hydrates: Occurrence, Distribution, and Detection*. AGU Monograph 124, pp. 41–52.
- Valentine, D.L., 2002. Biogeochemistry and microbial ecology of methane oxidation in anoxic environments: a review. *Antonie Van Leeuwenhoek* 81, 271–282.
- Valentine, D.L., Reeburgh, W.S., 2000. New perspectives on anaerobic methane oxidation. *Environ. Microbiol.* 2, 477–484.
- Villinger, H., Davis, E.E., 1987. A new reduction algorithm for marine heat flow measurements. *J. Geophys. Res.* 92, 12,846–12,856.
- Weimer, P., Buffler, R.T., 1992. Structural geology and evolution of the Mississippi Fan Fold Belt, Deep Gulf of Mexico. *AAPG Bull.* 76, 225–251.
- Westrich, J.T., Berner, R.A., 1984. The role of sedimentary organic matter in bacterial sulfate reduction: the G model tested. *Limnol. Oceanogr.* 29, 236–249.
- Whelan, J., Eglinton, L., Cathles II, I.L., Losh, S., Roberts, H., 2005. Surface and subsurface manifestations of gas movement through a N–S transect of the Gulf of Mexico. *Mar. Petr. Geol.* 22, 479–497.
- Winters, W.J., Dugan, B., Collett, T.S., 2008. Physical properties of sediments from Keathley Canyon and Atwater Valley, JIP Gulf of Mexico gas hydrates drilling program. *Mar. Petr. Geol.* 25, 896–905.
- Wood, W.T., Gettrust, J.F., Chapman, N.R., Spence, G.D., Hyndman, R.D., 2002. Decreased stability of methane hydrates in marine sediments owing to phase-boundary roughness. *Nature* 420, 656–660.
- Wood, W., Hart, P.E., Hutchinson, D.R., Dutta, N., Snyder, F., Coffin, R.B., Gettrust, J.F., 2008. Gas and gas hydrate distribution around seafloor seeps in Mississippi Canyon, northern Gulf of Mexico, using multi-resolution seismic imagery. *Mar. Petr. Geol.* 25, 952–959.
- Xu, W.Y., Ruppel, C., 1999. Predicting the occurrence, distribution, and evolution of methane gas hydrate in porous marine sediments. *J. Geophys. Res.* 104, 5081–5096.
- Yun, T.S., Narsilio, G.A., Santamarina, J.C., 2006. Physical characterization of core samples recovered from the Gulf of Mexico. *Mar. Petr. Geol.* 23, 893–900.
- Zhang, C.L., Pancost, R.D., Sassen, R., Qian, Y., Macko, S.A., 2003. Archaeal lipid biomarkers and isotopic evidence of anaerobic methane oxidation associated with gas hydrates in the Gulf of Mexico. *Org. Geochem.* 34, 827–836.